Room temperature ferromagnetic behavior in the hollandite-type titanium oxide

K. Noami,[1] Y. Muraoka,[1,2,a)] T. Wakita,[2] M. Hirai,[1,2] Y. Kato,[3] T. Muro,[3] Y. Tamenori,[3] and T. Yokoya[1,2]

[1]*Graduate School of Natural Science and Technology, Okayama University, 3-1-1 Tsushima-naka, Kita-ku, Okayama 700-8530, Japan*

[2]*Faculty of Science, Research Laboratory for Surface Science, Okayama University, 3-1-1 Tsushima-naka, Kita-ku, Okayama 700-8530, Japan*

[3]*Japan Synchrotron Radiation Research Institute (JASRI)/SPring-8, 1-1-1 Kouto, Sayo, Hyogo 679-5148, Japan*

(Received 15 October 2009; accepted 23 February 2010; published online 12 April 2010)

A hollandite-type $K_xTi_8O_{16}$ polycrystalline sample has been prepared and studied by magnetization, resistivity and x-ray photoelectron spectroscopy (XPS). Room temperature ferromagnetic behavior is observed in the magnetic hysteresis measurement. The sample shows a semiconductive temperature dependence in the resistivity measurement. Analysis of the Ti $2p_{3/2}$ core-level XPS spectrum indicates that the titanium ions have a mixed valence of Ti^{4+} and Ti^{3+}. In addition, the valence band spectrum reveals that the 3*d* electrons tend to localize on Ti^{3+} ions in the hollandite-type TiO_2 lattice. Also, analysis of the valence band spectrum shows that the prepared sample is a wide-gap oxide with a band gap of 3.6 eV. These results indicate that the present hollandite-type $K_xTi_8O_{16}$ sample can be classified as a TiO_2-based wide-gap semiconductor with Curie temperature above room temperature. Room temperature ferromagnetism (RTFM) decreases in the sample prepared under a strong reducing gas atmosphere, accompanied with the decrease in the resistivity. The results imply that the localized 3*d* electrons are responsible for the RTFM of the $K_xTi_8O_{16}$ sample. © *2010 American Institute of Physics*. [doi:10.1063/1.3369500]

I. INTRODUCTION

Titanium dioxide TiO_2 is a well-known material and has technologically important properties such as excellent optical transmittance in visible and near-infrared region, high refractive index and high dielectric constant. Recently, Matsumoto *et al.*[1] discovered room temperature ferromagnetism (RTFM) in Co-doped anatase TiO_2 thin film. Since that discovery, many materials with anatase (A) and rutile (R)-type TiO_2 structures have been developed in the form of film[2,3] and bulk[4,5] and their magnetic properties have been studied. So far, RTFM is observed when A and R-type TiO_2 are doped with transition metal ions,[2,4] and even when pure A and R-type TiO_2 are reduced[6,7] or implanted by Ar and N ions.[8] Now it is believed that TiO_2 has an additional physical property of ferromagnetism and is a potential material in an application field of spintronics devices. Concerning the mechanism of RTFM, it is considered that oxygen vacancies play an important role as the origin of RTFM.[3,5,9,10] It is also speculated that in some systems[11,12] carriers introduced into the lattice are essential for the appearance of RTFM. Although numerous studies have been claimed ferromagnetism above room temperature, the precise mechanism responsible for this behavior is subjected to debate.

It is very interesting and important to develop a new member of TiO_2-based RTFM because new material can provide valuable information for understanding the underlying physics of RTFM and also extend the possibility to develop the TiO_2-based devices for spintronics applications.

Hollandite-type TiO_2 is one of polymorphs in titanium dioxides and consists of a one-dimensional tunnel structure surrounded by interlinking of edge-shared TiO_6-octahedral units as shown in Figs. 1(a) and 1(b). The general formula of the hollandite-type titanium oxide is given as $A_xTi_8O_{16}$ ($0 \leq x \leq 2$), where A represents the ions such as Li^+, K^+, and Cs^+. The A cations occupy the tunnel, resulting in a mixed valence of titanium ions as Ti^{4+} and Ti^{3+} to preserve charge balance. Since interaction between the cations and hollandite-type TiO_2 framework is weak, the cations can be easily intercalated into and deintercalated from the tunnel with keeping intact the overall original structure. Because of the unique microporous feature, hollandite-type TiO_2 has been studied from the viewpoint of crystal structure[13] and application such as battery characteristics[14,15] and immobilization of radioactive elements.[16]

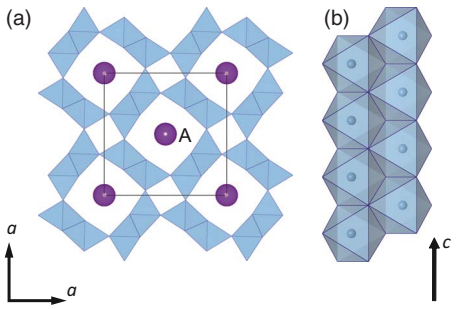

FIG. 1. (Color online) Crystal structure of hollandite-type $A_xTi_8O_{16}$ (A represents ions such as Li^+, K^+, and Cs^+) projected (a) along *a* axis and (b) along *c* axis. Each octahedron corresponds to the TiO_6 unit. Crystal structures were illustrated with the program VESTA (Ref. 27).

a)Electronic mail: ymuraoka@cc.okayama-u.ac.jp.

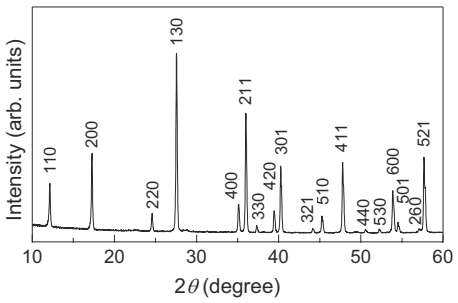

FIG. 2. Powder XRD pattern of $K_{1.46}Ti_8O_{16}$.

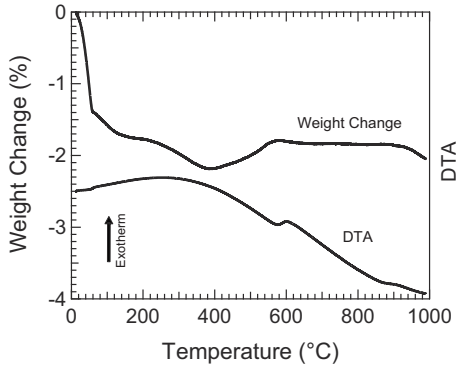

FIG. 3. TG-DTA curves of $K_{1.46}Ti_8O_{16}$ with a heating rate of 5 °C/min in flowing air.

The hollandite-type TiO_2 framework is composed of edge and corner-shared TiO_6 octahedron as A and R-type TiO_2 structures are composed. In addition, this material possesses the $3d$ electron in Ti^{3+} ion ($3d^1$) which is an important source of magnetic moment. These characteristics let us have expectation of an appearance of interesting physical properties such as RTFM as seen in A and R-type TiO_2 system. Until now, there are few reports on the physical properties of this material. In this work, we prepared hollandite-type $K_xTi_8O_{16}$ and studied the magnetic and electric properties and the electronic state of the sample by magnetization, resistivity, and x-ray photoelectron spectroscopy (XPS).

II. EXPERIMENT

Polycrystalline $K_xTi_8O_{16}$ sample was synthesized by solid-state reaction. Powders of K_2CO_3 and R-type TiO_2 were mixed with the mol ratio of $K_2CO_3:TiO_2=1:9$ and pressed into a pellet, then calcined at 1050 °C for 10 h under a H_2/Ar (5%/95%) gas atmosphere.[17] After calcination, dark-blue color sample was obtained. The prepared sample was examined by powder x-ray diffraction (XRD) using monochromated Cu $K\alpha$ radiation (Rigaku RINT-2000/PC). The unit-cell parameters were determined from the observed d-spacing by the least-squares method. Metal ratio of K/Ti in the sample was examined by energy dispersive x-ray (EDX) analysis. Both thermogravimetric and differential thermal analyses (TG-DTA) were done using a Rigaku TG8120. Magnetic measurements were performed using a superconducting quantum interference device magnetometer (Quantum Design MPMS). Resistivity measurements were carried out using a standard four-point probe method in a physical property measurement system (Quantum Design PPMS). XPS measurements were performed at SPring-8 BL27SU. Monochromated x-ray of 1300 eV was used for measurements and the total energy resolution was 370 meV. The $K_xTi_8O_{16}$ sample was fractured *in situ* before measurements. The Fermi level position was determined by measuring the Fermi edge of gold. All spectra were taken at room temperature.

III. RESULTS AND DISCUSSION

Figure 2 shows the powder XRD pattern of the prepared sample. By XRD analysis, this sample was found to be a single phase. The XRD pattern was similar to that of $K_{1.35}Ti_8O_{16}$ in the Joint Committee for Powder Diffraction Standard files (No. 47–690) and indexed with a tetragonal cell. The a and c parameters of the sample were determined to be $a=10.193$ Å and $c=2.966$ Å. These values are in good agreement with those of previous work.[14] Metal ratio in the sample was determined from EDX analysis to be K/Ti $=1.46/8$. Assuming that there is no oxygen vacancy in the sample, the chemical formula of the sample can be represented as $K_{1.46}Ti_8O_{16}$. The calculated average valence of titanium ions is +3.82, indicating the existence of low valence state of Ti^{3+} other than Ti^{4+}. Figure 3 shows a TG-DTA curve of the prepared sample measured at a heating rate of 5 °C/min in flowing air. A remarkable weight decrease was observed up to 120 °C. This weight loss was due to the desorption of absorbed water from the sample. The weight decreased slightly up to 390 °C, and then a weight increase started. The weight increased up to 580 °C, and then became almost constant. The weight decrease was again observed from 900 °C. On the other hand, an exothermic peak was observed at 600 °C. The obtained results are in good agreement with those in previous report.[17] The weight increase between 390 and 580 °C occurs due to oxidation of the sample.[17] Since the oxidized sample is found from XRD analysis to have a hollandite form, it is plausible that the oxygen is taken into the sample to compensate for the oxygen vacancies in the hollandite lattice. The results of TG-DTA measurements suggest the presence of certain amount of oxygen vacancies in the prepared sample.

Figure 4 shows the magnetic field dependence of magnetization (M-H) of $K_{1.46}Ti_8O_{16}$ measured at room temperature. The hysteresis with a coercive field of 80 Oe was observed, indicative of the ferromagnetic nature of the sample. At a high magnetic region, the magnetization showed a positive slop because of the paramagnetic contribution as seen in the inset of Fig. 4. These results indicate that ferromagnetic and paramagnetic natures coexist in the sample. Since Ti^{4+} ions have no $3d$ electron, the magnetic moment involved in the ferromagnetic and paramagnetic behaviors originates from unpaired $3d$ electrons in Ti^{3+} ions. A saturation magnetization for the ferromagnetic component was estimated by subtracting the paramagnetic component from M-H data to be 4×10^{-3} emu/g. The obtained value is similar to the values in V-doped TiO_2 powders,[18] Cr[5] and Co[19] -doped TiO_2 nanoparticles, and reduced A and R-type TiO_2 powders.[20] The saturation magnetization corresponds to 4×10^{-4} μ_B per Ti^{3+} ion. The relatively small saturation magnetization can

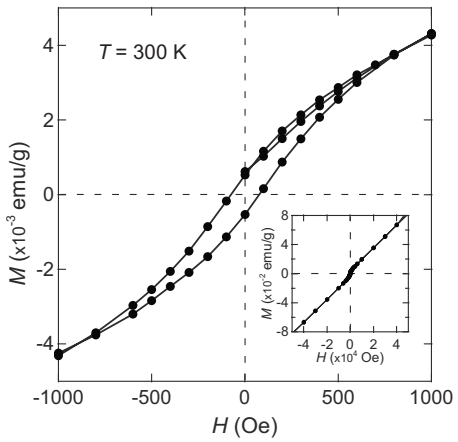

FIG. 4. Magnetic hysteresis (M-H) loop at room temperature for $K_{1.46}Ti_8O_{16}$. Inset represents M-H loop under the applied magnetic field from −50 000 to 50 000 Oe.

be explained on the hypothesis that a small fraction of Ti^{3+} ions is responsible for the observed ferromagnetism and a large fraction of Ti^{3+} ions is contributed to the paramagnetism. A mixture behavior of multiple magnetic interactions was reported in oxide diluted magnetic semiconductors such as Mn-doped ZnO nanoparticles.[21] The magnetic hysteresis still remains at 350 K, indicating that the Curie temperature of the sample is higher than 350 K. One may think the possibility of the impurity's contribution to the ferromagnetism. Such possibility can be excluded because no impurity phases are observed by XRD measurements, and also because even though a tiny amount of K–Ti–O related impurity phases are included in the sample such phases do not exhibit ferromagnetism at room temperature. Thus, we conclude that the observed RTFM can be attributed to be intrinsic due to the corporation of Ti^{3+} ions into the hollandite-type TiO_2 lattice.

Figure 5 shows the temperature dependence of resistivity ρ for the $K_{1.46}Ti_8O_{16}$ sample. The sample exhibits the semiconductive temperature dependence with negative $d\rho/dT$. The experimental data was analyzed by using the formula for variable range hopping (VRH) expressed as $\rho(T) = \rho(T_0)\exp(T_0/T)^{1/(d+1)}$, where T_0 is a characteristic temperature and d is the dimensionality of the system. As shown in

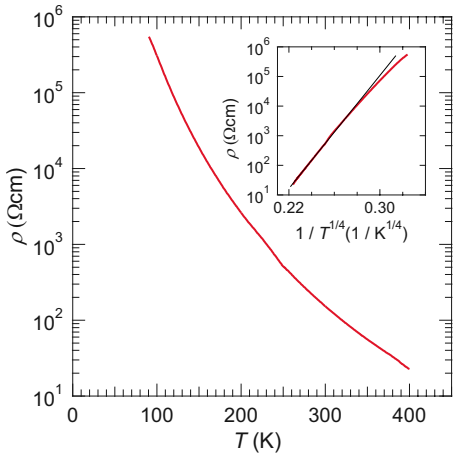

FIG. 5. (Color online) Temperature dependence of the resistivity for $K_{1.46}Ti_8O_{16}$. Inset represents the resistivity as a function of $T^{-1/4}$.

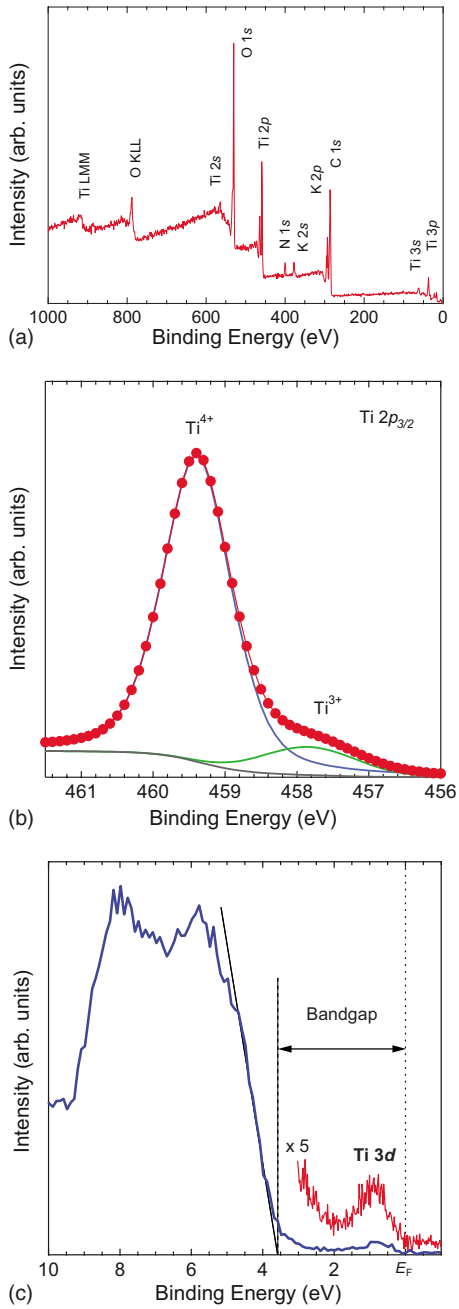

FIG. 6. (Color online) XPS spectra of (a) a wide scan range, (b) Ti $2p_{3/2}$ core-level and (c) valence band for $K_{1.46}Ti_8O_{16}$.

the inset of Fig. 5, fit with $d=3$ was successful at the temperature range between 190 and 380 K. This indicates that the dominant conduction mechanism is three-dimensional VRH. However, we should be careful about conclusion because the polycrystalline sample is used for the measurement. For a conclusion of the conduction mechanism, we need to carry out the measurement using single crystal sample.

In order to evaluate the valence state of the Ti ions in the sample, XPS measurements were performed. Figure 6(a) shows the wide scan of XPS spectrum of the sample. The three constituent elements, K, Ti, and O can be readily identified as carbon contamination can. No peak related to the magnetic impurity such as iron was observed within the de-

tection limit (0.1 at. %), supporting that the observed ferromagnetic behavior originates from $K_{1.46}Ti_8O_{16}$. Figure 6(b) shows the Ti $2p_{3/2}$ core-level spectrum of the sample. The spectrum showed a peak structure with a shoulder at lower binding energy. The peak was deconvoluted into two symmetric peaks; main peak was at the binding energy of 459.4 eV and the other small peak was at 457.9 eV. The main peak is attributed to the Ti^{4+} state. The small peak separated by 1.5 eV from Ti^{4+} state can be ascribed to the Ti^{3+} state.[22] There is no peak from Ti^{2+} state (peak separation from Ti^{4+} is more than 3 eV). This result indicates that the Ti ions take two kinds of valence state of Ti^{4+} and Ti^{3+}. The ratio of Ti^{4+}/Ti^{3+} is estimated from the peak area of Ti^{4+} and Ti^{3+} state to be 88/12 which corresponds to the average valence of Ti ions of +3.88. The estimated average valence of Ti ions is in good agreement with that from the EDX analysis. Figure 6(c) shows the valence band spectrum for the sample. The valence band spectrum showed a two-peak structure. A peak located at 8 eV is mainly due to the Ti $3d$ band and the other peak situated at 5.8 eV is mainly due to the O $2p$ band. The origin of the peak structures is examined by our resonant photoemission spectroscopy measurements (not shown in the paper). A small but distinct peak was observed at around 0.8 eV below the Fermi level. This peak originates from the Ti $3d$ state.[23] The presence of the Ti $3d$ state is consistent with the result that the Ti^{3+} state is observed in the Ti $2p_{3/2}$ core-level spectrum. The Ti $3d$ state had a narrow band width and no intensity at the Fermi level. This means that the $3d$ electrons tend to localize on the Ti^{3+} ions in the hollandite-type TiO_2 lattice. The localized character of the $3d$ electrons is seen in the result of resistivity measurement where the semiconducting behavior is observed. Such localized unpaired $3d$ electrons in Ti^{3+} ions can lead to the magnetic moment and a part of them must be contributed to the ferromagnetic behavior as mentioned in Fig. 4. From Fig. 6(c), we estimate the band gap of the sample. It is known that in TiO_2 the Fermi level is pinned just below the conduction band.[24] In this sample, assuming that the Fermi level is located at the bottom of the conduction band, the band gap can be estimated from the binding energy of the top of valence band to be 3.6 eV. This band gap is slightly larger compared with values of A and R-TiO_2 (3.2 and 3.0, respectively) and thus, $K_{1.46}Ti_8O_{16}$ is found to be classified in wide-gap oxides. Considering the results of magnetization and resistivity measurements, $K_{1.46}Ti_8O_{16}$ can be regarded as a new member of TiO_2-based wide-gap semiconductors with Curie temperature above room temperature.

It is interesting to see how the physical properties change when the sample preparation condition is changed. We prepared the sample in a preparation condition same as the sample which we mentioned above except a partial H_2 pressure during the calcination. The sample was calcined under a pure H_2 gas atmosphere (hereafter denoted as sample-H100). Figure 7 shows the thermogravimetric analysis (TGA) curve of sample-H100 together with that of the aforementioned $K_{1.46}Ti_8O_{16}$ sample prepared under the H_2/Ar (5%/95%) gas atmosphere (hereafter denoted as sample-H5) for comparison. In the figure, the TGA curves were normalized by the weight at 390 °C. Sample-H100 showed the

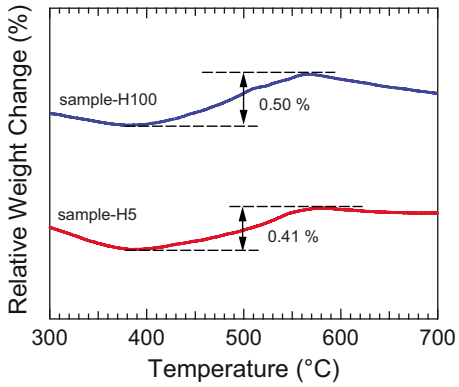

FIG. 7. (Color online) TGA curve of the sample prepared under a pure H_2 gas atmosphere (represented as sample-H100), together with the data of the sample prepared under a H_2/Ar (5%/95%) gas atmosphere (represented as sample-H5). The TGA curves were normalized by the weight at 390 °C.

weight increase because of oxidization between 390 and 570 °C, indicating the presence of oxygen vacancies in the sample. The weight increase was found to be 0.50%. The value is larger compared with the case for sample-H5 (0.41%). Since sample-H100 is prepared under a strong reducing gas atmosphere, larger number of oxygen vacancies can be introduced in the hollandite-type TiO_2 lattice for sample-H100. We measured the resistivity and magnetic hysteresis loop for sample-H100 and compared the results with those for sample-H5. Figure 8(a) shows the temperature dependence of resistivity for sample-H100 together with the data of sample-H5 (same as the data of Fig. 5). Sample-H100 shows a semiconducting behavior and is more conductive compared with sample-H5. The smaller resistivity suggests that the introduced oxygen vacancies play a role as n-type doping. An interesting change is observed in the magnetic hysteresis measurement. Figure 8(b) shows the magnetic hysteresis loop at room temperature for sample-H100 together with that for sample-H5 (same as the data of Fig. 4). As seen in the figure, paramagnetism was dominant for sample-H100 although the trace of the ferromagnetism was observed. A saturation magnetization for the ferromagnetic component estimated by subtracting the paramagnetic component was 1.5×10^{-3} emu/g. It is obvious that the ferromagnetism decreases compared with sample-H5. The result indicates that partial H_2 pressure during sample preparation is one of key parameters for the appearance of the ferromagnetic behavior. It is also found from the results that the ferromagnetism tends to suppress when the sample becomes conductive. This implies that the ferromagnetism stems from the localized $3d$ electrons in the hollandite-type TiO_2 lattice. This picture is different from the case in Co or Fe-doped TiO_2 (Refs. 11 and 12) where the $3d$ electron carriers induce ferromagnetism.

The origin of RTFM of the present hollandite-type $K_{1.46}Ti_8O_{16}$ is the critical issue to be solved. Our results imply that the localized $3d$ electrons are responsible for the ferromagnetism of $K_{1.46}Ti_8O_{16}$. In order to confirm the implication, we intend to study the microstructure of the sample by means of electron spin-resonance spectroscopy. The result will provide information on the origin of the magnetic moment in $K_{1.46}Ti_8O_{16}$. We also plan to do the measurements of

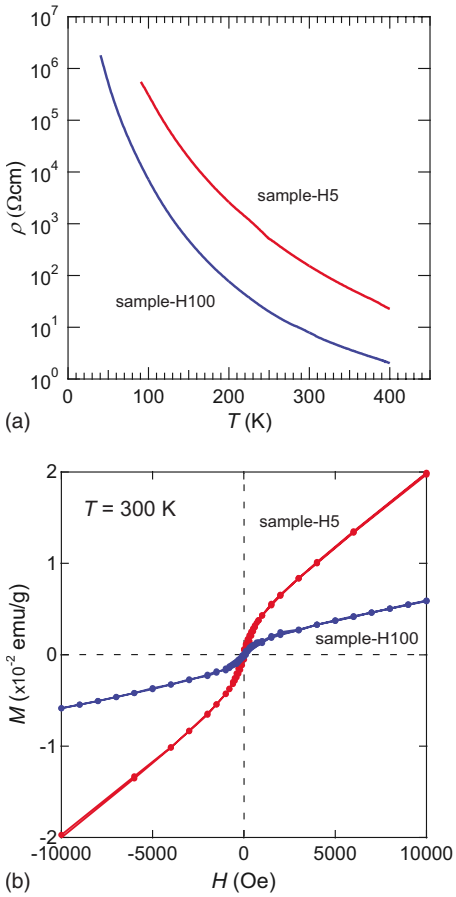

FIG. 8. (Color online) (a) Temperature dependence of the resistivity for sample-H100. Resistivity data of sample-H5 shown in Fig. 4 is plotted for comparison. (b) Magnetic hysteresis loop at room temperature for sample-H100 together with the data of sample-H5 shown in Fig. 3.

extended x-ray absorption fine structure and Raman scattering to examine the presence of titanium and/or oxygen vacancies in the sample which have been suggested to be critical components of RTFM in A and R-type TiO_2.[3,5,9,10,25,26] On the other hand, from the viewpoint of applications, it is important to prepare $K_xTi_8O_{16}$ thin films and investigate the magnetic properties. In our preliminary work, we succeed in preparing a $K_xTi_8O_{16}$ thin film epitaxially grown on a sapphire substrate and find that the film shows ferromagnetic behavior at room temperature. Knowledge from the studies in $K_xTi_8O_{16}$ would not only help understand the underlying physics of RTFM in the TiO_2-based system but also be useful toward developing the TiO_2-based devices for spintronics applications. Finally, we comment on the way to develop new TiO_2-based room temperature ferromagnets. There are many polymorphs in TiO_2 such as ramsdellite and bronze. The present hollandite-type TiO_2 is the only one of them. Our results indicate that the research on polymorphs would be promising for developing new TiO_2-based room temperature ferromagnets.

IV. CONCLUSIONS

In summary, we have synthesized polycrystalline hollandite-type $K_{1.46}Ti_8O_{16}$ and studied the magnetic and electric properties and the electronic state of the sample. Ferromagnetic behavior is observed at room temperature in the magnetic hysteresis measurement. The sample shows the semiconducting behavior in the resistivity measurement. XPS measurements indicate that the Ti ions take a mixed valence of Ti^{4+} and Ti^{3+}. The valence band spectrum reveals that the unpaired $3d$ electrons tend to localize on Ti^{3+} ions in the hollandite-type TiO_2 lattice. Analysis of the valence band spectrum indicates that $K_{1.46}Ti_8O_{16}$ is a wide gap oxide with the band gap of 3.6 eV. RTFM decreases in the sample prepared under a strong reducing gas atmosphere, accompanied with the decrease in the resistivity. The results imply that the localized $3d$ electrons are responsible for the ferromagnetism of $K_{1.46}Ti_8O_{16}$.

ACKNOWLEDGMENTS

We thank J. Takada and T. Fujii for XRD and TG-DTA curve measurements and EDX analysis, N. Hanasaki for resistivity measurements, and Z. Hiroi, K. Oshima, and T. Kambe for magnetization measurements. This research was supported by JST, CREST and The Ministry of Education, Culture, Sports, Science, and Technology, Japan.

[1] Y. Matsumoto, M. Murakami, T. Shono, T. Hasegawa, T. Fukumura, M. Kawaski, P. Ahmet, T. Chikyow, S. Y. Koshihara, and H. Koinuma, Science **291**, 854 (2001).
[2] N. H. Hong, J. Sakai, W. Prellier, A. Hassini, A. Ruyter, and F. Gervais, Phys. Rev. B **70**, 195204 (2004).
[3] J. M. D. Coey, M. Venkatesan, and C. B. Fitzgerald, Nature Mater. **4**, 173 (2005).
[4] L. Sangaletti, M. C. Mozzati, P. Galinetto, C. B. Azzoni, A. Speghini, M. Bettinelli, and G. Calestani, J. Phys.: Condens. Matter **18**, 7643 (2006).
[5] J. D. Bryan, S. A. Santangelo, S. C. Keveren, and D. R. Gamelin, J. Am. Chem. Soc. **127**, 15568 (2005).
[6] S. D. Yoon, Y. Chen, A. Yang, T. L. Goodrich, X. Zuo, D. A. Arena, K. Ziemer, C. Vittoria, and V. G. Harris, J. Phys.: Condens. Matter **18**, L355 (2006).
[7] N. H. Hong, J. Sakai, N. Poirot, and V. Brizé, Phys. Rev. B **73**, 132404 (2006).
[8] M. M. Cruz, R. C. D. Silva, N. Franco, and M. Godinho, J. Phys.: Condens. Matter **21**, 206002 (2009).
[9] A. Kaminski and S. D. Sarma, Phys. Rev. Lett. **88**, 247202 (2002).
[10] D. Kim, J. Hong, Y. R. Park, and K. J. Kim, J. Phys.: Condens. Matter **21**, 195405 (2009).
[11] H. Toyosaki, T. Fukumura, Y. Yamada, K. Nakajima, T. Chikyow, T. Hasegawa, H. Koinuma, and M. Kawasaki, Nature Mater. **3**, 221 (2004).
[12] T. Hitosugi, G. Kinoda, Y. Yamamoto, Y. Furubayashi, K. Inaba, Y. Hirose, K. Nakajima, T. Chikyow, T. Shimada, and T. Hasegawa, J. Appl. Phys. **99**, 08M121 (2006).
[13] T. Vogt, E. Schweda, C. Wüstefeld, J. Strähle, and A. K. Cheetham, J. Solid State Chem. **83**, 61 (1989).
[14] M. Latroche, L. Brohan, R. Marchand, and M. Tournoux, J. Solid State Chem. **81**, 78 (1989).
[15] L. D. Noailles, C. S. Johnson, J. T. Vaughey, and M. M. Thackeray, J. Power Sources **81–82**, 259 (1999).
[16] H. Abe, A. Satoh, K. Nishida, E. Abe, T. Naka, M. Imai, and H. Kitazawa, J. Solid State Chem. **179**, 1521 (2006).
[17] M. Watanabe, Y. Komatsu, T. Sasaki, and Y. Fujiki, J. Solid State Chem. **92**, 80 (1991).
[18] Z. M. Tian, S. L. Yuan, S. J. Yuan, H. Y. Xie, J. H. He, Y. Q. Wang, K. L. Liu, and S. Y. Yin, Solid State Commun. **146**, 522 (2008).
[19] D. Pan, G. Xu, L. Lv, Y. Yong, X. Wang, J. Wan, and G. Wang, Appl. Phys. Lett. **89**, 082510 (2006).
[20] Q. Zhao, P. Wu, B. L. Li, Z. M. Lu, and E. Y. Jiang, J. Appl. Phys. **104**, 073911 (2008).
[21] O. D. Jayakumar, H. G. Salunke, R. M. Kadam, M. Mohapatra, G.

Yaswant, and S. K. Kulshreshtha, Nanotechnology **17**, 1278 (2006).
[22]A. R. Gonzálenz-Elipe, G. Munuera, J. P. Espinos, and J. M. Sanz, Surf. Sci. **220**, 368 (1989).
[23]A. Fujimori, I. Hase, M. Nakamura, H. Namatame, Y. Fujishima, and Y. Tokura, Phys. Rev. B **46**, 9841 (1992).
[24]I. Takahashi, D. J. Payne, R. G. Palgrave, and R. G. Egdell, Chem. Phys. Lett. **454**, 314 (2008).
[25]H. S. Ahn, S. Han, and C. S. Hwang, Appl. Phys. Lett. **90**, 252908 (2007).
[26]H. Peng, J. Li, S. S. Li, and J. B. Xia, Phys. Rev. B **79**, 092411 (2009).
[27]K. Momma and F. Izumi, J. Appl. Crystallogr. **41**, 653 (2008).